

# Designer epigenome modifiers enable robust and sustained gene silencing in clinically relevant human cells

Tafadzwa Mlambo<sup>1,2,3,4</sup>, Sandra Nitsch<sup>1,2,4</sup>, Markus Hildenbeutel<sup>1,2</sup>, Marianna Romito<sup>1,2,4</sup>, Maximilian Müller<sup>1,2,4</sup>, Claudia Bossen<sup>2</sup>, Sven Diederichs<sup>5,6</sup>, Tatjana I. Cornu<sup>1,2</sup>, Toni Cathomen<sup>1,2,6</sup> and Claudio Mussolino<sup>1,2,\*</sup>

<sup>1</sup>Institute for Transfusion Medicine and Gene Therapy, Medical Center – University of Freiburg, Freiburg, Germany, <sup>2</sup>Center for Chronic Immunodeficiency, Medical Center – University of Freiburg, Freiburg, Germany, <sup>3</sup>Spemann Graduate School of Biology and Medicine (SGBM), University of Freiburg, Freiburg, Germany, <sup>4</sup>Faculty of Biology, University of Freiburg, Freiburg, Germany, <sup>5</sup>Division of Cancer Research, Department of Thoracic Surgery, Medical Center – University of Freiburg & German Cancer Consortium (DKTK), Freiburg, Germany & Division of RNA Biology & Cancer, German Cancer Research Center (DKFZ), Heidelberg, Germany and <sup>6</sup>Faculty of Medicine, University of Freiburg, Freiburg, Germany

Received October 17, 2017; Revised February 23, 2018; Editorial Decision February 26, 2018; Accepted February 27, 2018

## ABSTRACT

**Targeted modulation of gene expression represents a valuable approach to understand the mechanisms governing gene regulation. In a therapeutic context, it can be exploited to selectively modify the aberrant expression of a disease-causing gene or to provide the target cells with a new function. Here, we have established a novel platform for achieving precision epigenome editing using designer epigenome modifiers (DEMs). DEMs combine in a single molecule a DNA binding domain based on highly specific transcription activator-like effectors (TALEs) and several effector domains capable of inducing DNA methylation and locally altering the chromatin structure to silence target gene expression. We designed DEMs to target two human genes, *CCR5* and *CXCR4*, with the aim of epigenetically silencing their expression in primary human T lymphocytes. We observed robust and sustained target gene silencing associated with reduced chromatin accessibility, increased promoter methylation at the target sites and undetectable changes in global gene expression. Our results demonstrate that DEMs can be successfully used to silence target gene expression in primary human cells with remarkably high specificity, paving the way for the establishment of a potential new class of therapeutics.**

## INTRODUCTION

Gene expression is a tightly regulated mechanism that is the foundation for creating the transcriptional diversity that leads to the formation of highly specialized cells and tissues in an organism (1). DNA methylation at CpG dinucleotides is a crucial factor in regulating gene expression and aberrant DNA methylation often leads to disease (2,3). Epigenetic drugs have already been used to reverse epigenetic landscapes associated with cancer or neurological disorders but their lack of selectivity is a serious drawback (4–6). The ability to precisely change the epigenome, a concept named targeted epigenome editing, is thereby tempting. This approach aims to deposit or remove epigenetic marks, such as DNA methylation or post-translational histone modifications, to locally alter the chromatin structure and resulting in increased or reduced target gene expression (7). Typically, designer transcription factors (DTFs) are exploited to up- or down-regulation genes in a targeted manner (8). DTFs are generally engineered with DNA binding moieties, that define target specificity, fused to an effector domain either for gene activation, such as the tripartite activator VP64-p65-Rta (VPR) (9), or for gene repression as the Krüppel-associated box (KRAB) (10). Despite their efficiency, these systems generally allow only transient gene regulation particularly in dividing cells or proliferating tissues. Sustained control of gene expression is still challenging (11) and it may either require the repeated application of the synthetic transcriptional regulator (12) with the risk of potential immune reactions, or its continuous expression by means of potentially mutagenic integrating vectors (13).

\*To whom correspondence should be addressed. Tel: +4976127077738; Fax: +4976127077749; Email: claudio.mussolino@uniklinik-freiburg.de  
Present address: Claudio Mussolino, Center for Chronic Immunodeficiency, Medical Center – University of Freiburg, Freiburg, 79106, Germany.

Alternatively, RNA interference can be exploited for post-transcriptional gene silencing (14) but it harbors a non-trivial risk of oversaturating cellular pathways for the processing of small RNA molecules (15) that hampers its use for clinical applications.

In the last decade, alternative methods to sustainably block gene expression have been explored. Genome engineering using designer nucleases has been largely used to genetically inactivate target genes for multiple applications (16). A seminal study has recently shown the potential of applying genome editing to human gene therapy by creating immune cells resistant to human immunodeficiency virus (HIV) infection (17). However, the genotoxic potential and careful evaluation of the risk/benefit ratio are important aspects to consider in order to make these technologies amenable at improving human quality of life (18).

Targeted epigenome editing is emerging as a promising alternative approach to overcome the limitations of current technologies. While maintaining the positive aspect of the 'hit-and-run' nature of genome editing, targeted epigenome editing is reversible and off-target activity may be less deleterious. A number of studies have demonstrated that targeted deposition or removal of epigenetic marks on DNA or histones have a direct impact on target gene expression (19,20). Recently, engineered TALE- and CRISPR-based epigenome editors have shown high specificity and tolerability in surrogate cellular models and robust silencing activity in primary T cells, though at a reporter locus integrated in their genome (21). Notwithstanding these data, efficacy of epigenome editing in controlling the expression of endogenous genes in clinically relevant primary human cells remains elusive. Moreover, to properly assess the potential of epigenome editing for future clinical translation, a thorough profiling of off-target effects in clinically relevant cells is still lacking.

We have established a novel platform to sustainably silence the expression of target genes in a hit-and-run approach. We merged the high specificity of TALE domains with a combination of different epigenome editors in a single molecule that we have named designer epigenome modifier (DEM). We demonstrate that DEMs are highly effective in inducing stable gene silencing in primary T lymphocytes by altering the DNA methylation and chromatin accessibility at the target site. As a proof-of-concept, we have targeted the promoter regions of two human genes relevant for the development of novel HIV therapeutics, *CCR5* and *CXCR4*. By a thorough analysis of off-target effects, we demonstrate that DEM can permanently alter target gene expression with remarkable specificity, supporting the future use of epigenome editing to treat human disorders.

## MATERIALS AND METHODS

### Plasmids construction

Transcription activator-like effector (TALE)-based DNA binding domains were generated as previously described (22). Six and four target sites were chosen in a window of 350 bp centered around the transcription start site of *CCR5* and *CXCR4* genes respectively, fulfilling the following criteria: (i) starting with a 5'T; (ii) proximity to known *cis*-regulatory elements and (iii) in a region of open chromatin

in human CD4+ T cells as shown by the tracks for DNase I hypersensitivity sites available in the UCSC Genome Browser database (<http://genome.ucsc.edu/>). The TALE-based DNA binding domains targeting the sequences of choice were cloned into an expression vector containing our previously optimized TALE scaffold (23) ( $\Delta 135/+17$ ) fused to different effector domains as follows: VP16 for designer transcription activator (DTA), KRAB for designer transcription repressor (DTR), a previously published fusion of the C-terminal region of the human DNA methyltransferase 3A (DNMT3A) linked to the C-terminal region of the murine Dnmt3-like (Dnmt3L) protein (24) for designer methyltransferase (DMT) with the N-terminal addition of the KRAB domain for designer epigenome modifiers (DEM). An expression vector lacking the KRAB domain and including the inactivating E752A amino acid substitution in the catalytic site of the DNMT3A (25) was generated to obtain inactive or 'dead' designer epigenome modifiers (dDMT). To generate the Firefly Luciferase and EGFP-based *CCR5* reporters, a region of the *CCR5* promoter containing the chosen target sites was PCR amplified from genomic DNA extracted from Jurkat cells using the primers indicated in Supplementary Table S7 and cloned into an expression vector containing Firefly Luciferase or a third-generation lentiviral vector in which EGFP is under the control of a minimal CMV promoter (Figure 1A) respectively. All the corresponding plasmids are available from the authors upon request.

### Cell lines and primary T cell culture

HEK293T cells were maintained in Dulbecco's Modified Eagle Medium (DMEM) supplemented with 10% Fetal Calf Serum (FCS) (PAA), 1% Penicillin/Streptomycin (GE Healthcare) and 1% sodium pyruvate (Biochrom). Cells were cultured at 37°C and 5% CO<sub>2</sub> in a humidified incubator. In order to generate the HEK293T-EGFP reporter cell line HEK293T cells were transduced with a lentiviral vector containing the reporter construct showed in Figure 1A at an MOI of 0.03. HEK293T-EGFP single clones were isolated after 17 days via fluorescence-activated cell sorting (FACS) using the MoFlo Astrios Cell Sorter (Beckman Coulter). Human CD4+ T cells were obtained from the peripheral blood mononuclear cells (PBMCs) of healthy donors by Ficoll density gradient centrifugation followed by human CD4+ T Cell Isolation Kit (Miltenyi Biotec) separation according to the manufacturer's instructions. The cells were activated for 3 days using magnetic beads conjugated with antibodies against CD2, CD3 and CD28 (Miltenyi Biotec) at a 2:1 cell to bead ratio and kept at a density of  $1.3 \times 10^6$  cells/cm<sup>2</sup> and  $2.5 \times 10^6$  cells/ml in X-VIVO 15 Chemically Defined Serum-free Hematopoietic Cell Medium (Lonza). To maintain the cells in culture long-term the activation was repeated every seven days and beads were removed after 3 days of activation. After bead removal, growth medium was supplemented with 20 U/ml interleukin 2 (Miltenyi Biotec).

### Delivery procedures

Constructs were delivered into the reporter cell line either as plasmid DNA or as *in vitro* transcribed mRNA. DNA

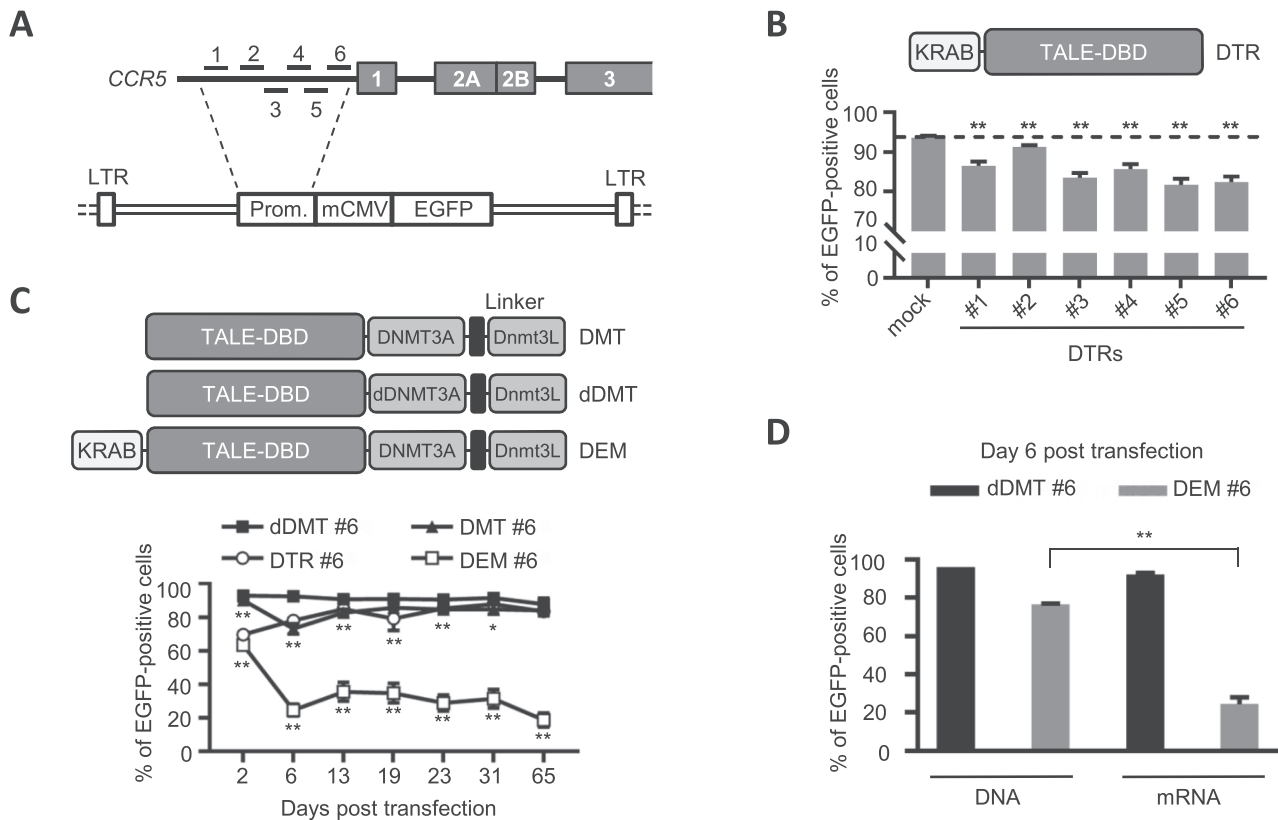


**Figure 1.** Stable gene silencing induced by DEMs as compared to DTRs. (A) Schematics of the *CCR5* gene and the lentiviral reporter. A 320 bp region from the endogenous *CCR5* promoter was fused to a minimal CMV promoter driving the expression of EGFP creating a lentiviral reporter which was used to generate a stable cell line in HEK293T cells (HEK293T-EGFP). Target sites #1 to #6 targeting the + or – DNA strand are indicated. Grey boxes represent *CCR5* exons. (B) Functional assessment of the designer transcriptional repressors (DTRs). The structure of the DTR is depicted (top) with a TALE DNA-binding domain targeting *CCR5* (positions #1 to #6) fused to a KRAB repressor. Transfections were carried out in the HEK293T-EGFP reporter cell line and EGFP expression measured via flow cytometry after 7 days. mock: shuttle plasmid containing a KRAB repressor domain but lacking a *CCR5*-specific DNA-binding domain. The dashed line denotes the reference value in the mock-treated cells (mean  $\pm$  S.E.M., experiments were performed at least three times in duplicate). Statistical significance calculated with a two-tailed, homoscedastic Student's *t*-test (\*\* $P < 0.01$ ). (C) Functionality of the DEMs in the HEK293T-EGFP reporter cell line. Structure of the construct used is shown on top. The TALE-based DNA binding domain targeting the position #6 in the *CCR5* promoter was included in the different constructs depicted encoding for designer methyltransferase (DMT), its inactive counterpart (dDMT) and the designer epigenome modifier (DEM). Transfections were performed with *in vitro* transcribed mRNA. Activity of the different effectors resulted in reduction of the EGFP positive cells over time as measured via flow cytometry. dDMT targeting position #6 was used as a negative control (mean  $\pm$  S.E.M., experiments were performed at least three times in duplicate). Statistical significance calculated with a two-tailed, homoscedastic Student's *t*-test (\*\* $P < 0.01$ ). (D) Route of delivery impacts on DEM's activity. Six days following delivery in HEK293T-EGFP reporter cell line either in form of plasmid DNA or as *in vitro* transcribed mRNA, DEM #6 activity was measured as reduction in the amount of EGFP+ cells via flow cytometry (mean  $\pm$  S.E.M.). Statistical significance calculated with a two-tailed, homoscedastic Student's *t*-test (\*\* $P < 0.01$ ).

transfections were carried out using polyethylenimine (PEI) and  $1.3 \times 10^5$  HEK293T cells or HEK293T-EGFP reporter cells respectively following manufacturer instructions. In the activation experiments shown in Supplementary Figure S1, the co-transfection mix included 400 ng of each effector, 15 ng of the Luciferase reporter and 5 ng of a Renilla Luciferase plasmid. Twenty-four hours post transfection, DTA activity was measured via Dual Luciferase assay (Promega) following the manufacturer's instructions and Renilla Luciferase was used to normalize the Firefly Luciferase signal. For the reactivation experiments shown in Supplementary Figure S5, HEK293T-EGFP reporter cells in which the EGFP was silenced, were isolated using fluorescence activated cell sorting (FACS) nineteen days after the delivery of DEM #6 to obtain EGFP-negative cells. For the DTA and 5-AZA reactivation,  $1.3 \times 10^5$  cells per well were seeded on a 24-well or 6-well plate respectively. Transfec-

tions were carried out in triplicate with a transfection mix containing 1150 ng of the DTA #6 or the corresponding control plasmid lacking the DNA binding domain and 100 ng of a reporter plasmid encoding for mCherry to monitor for transfection efficiency. For the 5-AZA reactivation the EGFP-negative cells were either treated daily with 10  $\mu$ M of 5-Aza-2'-deoxycytidine (5-AZA) freshly prepared in culture medium or left untreated. Flow cytometry was used to measure the extent of DTA- or 5-AZA-mediated reactivation of EGFP signal three and six days post-delivery/treatment using the Accuri C6 (BD Biosciences) and data analysed using the Accuri C6 software (BD Biosciences). Delivery of mRNA was preceded by *in vitro* transcription of the corresponding mRNA encoding for the different effectors. Briefly, plasmid DNA containing the different TALE-based effectors was linearized using the PspOMI restriction enzyme and 1  $\mu$ g of the linearized plasmid was used for *in vitro*

transcription using the mMessage mMachine T7 Ultra kit (Thermo Fisher Scientific) according to the manufacturer's instructions. Transfections of *in vitro* transcribed mRNA in the HEK293T-EGFP reporter cells line were carried out with 2  $\mu$ g of mRNA using Lipofectamine 2000 (Thermo Fisher Scientific) and  $1.3 \times 10^5$  cells following the manufacturer's instructions. Delivery in primary human lymphocytes was achieved via nucleofection, 3 days post activation using the 4D Nucleofector X device and the P3 Primary Cell 4D Nucleofector X kit (Lonza) following the manufacturer's instructions. In brief, prior to nucleofection the magnetic beads for activation were removed. Nucleofection was carried out with  $2.5 \times 10^6$  cells and 5  $\mu$ g of mRNA according to the manufacturer's protocol for stimulated human T cells. Following nucleofection, the cells were cultured in X-VIVO 15 medium supplemented with IL2 (final concentration 20 U/ml) and passaged every three days post nucleofection to a density of  $0.3 \times 10^6$  cells/cm<sup>2</sup> and  $0.5 \times 10^6$  cells/ml. Cells were harvested on day 7 and day 21 for quantitative RT-PCR and flow cytometry analysis. For the flow cytometry analysis the anti-CCR5 3A9 (BD Biosciences) and anti-CXCR4 12G5 (BioLegend) monoclonal antibodies were used. Flow cytometry was carried out using the FACS Canto II (BD Biosciences) and data analysed using FlowJo (FlowJo LLC).

### Gene expression analysis

Cells were harvested on the indicated days and total RNA isolated using the RNeasy Mini kit (Qiagen) according to the manufacturer's instructions. Reverse transcription was carried out using 500 ng of RNA and the QuantiTect Reverse Transcription kit (Qiagen) following the manufacturer's instructions. For the quantitative RT-PCR analysis, 50 ng of cDNA were used with the TaqMan Gene Expression Master Mix (Thermo Fisher Scientific). The TaqMan Gene Expression Assays used are indicated in Supplementary Table S8. Analysis was performed in triplicate using the StepOnePlus Real-Time PCR System (Applied Biosystems). Gene expression was calculated using the  $2^{-\Delta C_t}$  method normalized to the housekeeping gene B2M and expressed relative to control samples. Whole transcriptome analysis was performed via RNA sequencing (RNA seq). Briefly, primary human lymphocytes were nucleofected in triplicate either with mRNA encoding for the DEM #6 or its corresponding control (dDMT #6). Four days later, total RNA was extracted and whole transcriptome sequencing outsourced at the sequencing facility of the Center for Genomics and Transcriptomics (CeGaT). Bioinformatic analysis included demultiplexing of the sequencing reads using Illumina CASAVA (2.17) and adaptor trimming with Skewer (26) (version 0.1.116). Trimmed raw reads were aligned to the human reference genome (hg19) using STAR (27) (version 2.5.1). The R package DESeq2 was used to normalize the read counts which were further analyzed with Microsoft Excel.

### Chromatin Immunoprecipitation (ChIP) assay followed by quantitative RT-PCR

One million cells were fixed for 10 minutes in 1% formaldehyde in culture medium. Formaldehyde was quenched for

10 min with 1.5 M glycine then the cells were washed with ice-cold PBS. 15  $\mu$ l Protein G Dynabeads (Thermo Fisher Scientific) were blocked with 0.5% BSA (w/v) in PBS. Magnetic beads were bound with 3  $\mu$ g of a ChIP-grade antibody against H3K9me3 (Abcam). Crosslinked cells were lysed directly in sonication buffer (10 mM Tris-HCl pH 8.0, 0.5% SDS, 5 mM EDTA) and incubated 10 min on ice. Sonication was performed for 5 cycles at 10 s each on ice (sonication amplitude 18%) with 1 min pauses on ice between cycles. Lysates were cleared by centrifugation and dilution buffer (10 mM Tris-HCl pH 8.0, 1.25% Triton X-100, 0.125% Na-deoxycholate, 187.5 mM NaCl) and sonicated chromatin were mixed in a 4:1 ratio. Lysates were either retained as the input or incubated overnight at 4°C with the previously prepared magnetic beads. Beads were washed once with RIPA (50 mM Tris-HCl pH 8.0, 150 mM NaCl, 0.1% SDS, 0.1% Na-deoxycholate, 1% Triton X-100, 1 mM EDTA), once with RIPA 500 (50 mM Tris-HCl pH 8.0, 500 mM NaCl, 0.1% SDS, 0.1% Na-deoxycholate, 1% Triton X-100, 1 mM EDTA), once with LiCl wash (10 mM Tris-HCl pH 8.0, 250 mM LiCl, 0.5% NP-40, 0.5% Na-deoxycholate, 1 mM EDTA) and finally twice with TE (10 mM Tris pH 8.0, 1 mM EDTA). Bound complexes were eluted from the beads in elution buffer (10 mM Tris-HCl pH 8.0, 0.5% SDS, 300 mM NaCl, 5 mM EDTA) for 30 min at 65°C with shaking. Crosslinks were reversed overnight at 65°C. RNA and protein were digested in the supernatant using RNase A and Proteinase K. DNA was purified using the ChIP DNA Clean & Concentrator kit (Zymo Research) and eluted in 60  $\mu$ l of elution buffer. RT-PCR analysis was carried out using 3  $\mu$ l of DNA and the QuantiTect SYBR Green PCR kit (Qiagen) in duplicate or triplicate. The primers used are indicated in Supplementary Table S7. The percentage of input was calculated using the  $2^{-\Delta C_t}$  method using the input as a normalizer then expressed relative to the negative control site actin. The UNTR5 site was used as a positive control.

### Computational prediction of off-target sites

Potential off-target sites were predicted for the TALE-based DNA binding domain targeting the site #6 in the CCR5 promoter using the online tool TAL Effector Targeter (28) (<https://tale-nt.cac.cornell.edu/node/add/single-tale>). The top-10 predicted off-target sites are shown in Table 1. To identify all potential genomic sites harboring up to three mismatches as compared to the on-target sequence (listed in Supplementary Table S3), we used the COSMID online tool (29) (<https://crispr.bme.gatech.edu/>) using the following sequence as input: TGACCATATACTTATGT-CANNN.

### Bisulfite conversion of genomic DNA followed by Sanger sequencing or next generation sequencing

Genomic DNA was extracted using the QIAamp DNA Blood Mini kit (Qiagen) and bisulfite conversion performed using the EZ DNA Methylation Gold kit (Zymo Research) according to the manufacturer's instructions. Bisulfite converted DNA was PCR-amplified using the PyroMark PCR kit (Qiagen) then purified using the QIAquick PCR Purification kit (Qiagen). For low-throughput Sanger sequenc-

**Table 1.** List of potential off-target sites identified with TAL Effector Nucleotide Targeter 2.0

ID	Chromosome	Strand	Gene	Mismatches	Score	Start Position	Target Sequence	Distance from TSS (bp)	COSMID prediction <sup>1</sup>
0	3	+	<i>CCR5</i>	0	4.98	46,411,596	TGACCATATACCTTATGTCA	19	
1	7	+	<i>LOC101927668</i>	2	6.24	20,121,800	TAACCATATACCTTATCTCA	42'968	ID #35
2	4	+	<i>Intergenic</i>	1	7.31	165,401,212	TGAACATATACCTTATGTCA	n/a	ID #1
3	18	+	<i>YES1</i>	2	8.04	779,684	TGACCATATACCTTATCTCA	32'626	ID #40
4	17	+	<i>Intergenic</i>	3	8.24	8,563,008	TCACCATATACATATATCA	n/a	ID #580
5	20	+	<i>Intergenic</i>	3	8.24	12,726,816	TCACCATATACATATATCA	n/a	ID #582
6	5	+	<i>Intergenic</i>	3	8.24	97,609,784	TCACCATATACATATATCA	n/a	ID #581
7	12	+	<i>TEAD4</i>	2	8.36	3,076,665	TGAACATATACCTTATCTCA	8'186	ID #36
8	5	+	<i>LOC101927421</i>	3	8.63	124,565,833	TAACCATATATTTATATCA	193'308	ID #545
9	X	-	<i>Intergenic</i>	3	8.63	112,150,169	TAACCATATATTTATATCA	n/a	ID #544
10	2	-	<i>NYAP2</i>	3	8.9	226,408,801	TAGCCATATACCTTATATCA	143'199	ID #440

<sup>1</sup> As shown in Supplementary Table S3.

ing, PCR amplicons were cloned into the pJET1.2 plasmid (Thermo Fischer Scientific) then sequenced with the pJET1.2 forward and reverse sequencing primers (Supplementary Table S7). Methylation analysis was carried out using the software QUMA. For next generation bisulfite sequencing, libraries were constructed from PCR amplicons using the NEBNext Ultra II DNA Library Prep Kit for Illumina (NEB, E7645) and quantified using the ddPCR Library Quantification Kit for Illumina TruSeq (Biorad, #186–3040). All samples were sequenced on an Illumina MiSeq platform with a MiSeq Reagent Micro Kit v2, 300 cycles (Illumina, MS-103-1002). Depending on the amplicon size, paired-end reads were either merged using Fast Length Adjustment of SHort reads (FLASH) (30) or processed individually and mapped to the corresponding amplicon sequences using the Burrows-Wheeler Aligner (BWA) (31). Possible methylation sites (CGs) were identified within the amplicon sequences and mapped reads were analyzed at these positions to retrieve events of bisulfite conversion indicative of CpG methylation. The extent of CpG methylation for each position investigated is calculated as the ratio between the mapped reads showing a cytosine (C) and the total number of mapped reads. The extent of CpG methylation reported in the histogram in Figure 4h is a result of the average level of methylation of all cytosine residues present in the indicated amplicon.

#### ATAC-Seq analysis

Cells were harvested on day 12 or 13 and ATAC-Seq was performed as described (32) with minor changes. In brief, after lysis cells were spun for 30 min at 300 g and 'tagmentation' (transposase-based fragmentation) was performed for 1 h at 37°C with the Nextera DNA Sample Preparation Kit (Illumina). Tagmented DNA was purified using ChIP DNA clean and concentrator columns (ZymoResearch). Library fragments were amplified with NEBNext Ultra II Q5 Master Mix and custom Nextera PCR primers. The number of cycles was determined by quantitative PCR as described (32). Libraries were purified and size-selected with AMPure XP beads (Beckman Coulter) and sequenced on a HiSeq 2000 system as single reads. Reads were aligned to hg19 with Bowtie software (Johns Hopkins University) with the parameter  $-m 1$ . Data were analyzed with the HOMER suite of tools (hypergeometric optimization of motif enrichment). Tag directories were generated with the parameter  $-tbp 1$ , which removed most of the 'reads' arising

from mitochondrial DNA. Two biological replicates were performed. Circos software package was used for visualization; the replicates were combined. To identify differences in region of open chromatin, the regions of open chromatin from Th1 cells (<https://www.encodeproject.org/experiments/ENCSR000EQE/>) were annotated with the tag directories. Potential off-targets were determined as those sites showing 3-fold differences between the control and modified cells in both replicates and a minimum of four normalized tags in control cells.

#### Statistical analysis

All experiments have been performed at least three times in triplicates unless otherwise specified in the corresponding figure legends. Error bars represent standard error of mean (S.E.M.). Statistical significance was determined using a two-tailed, homoscedastic Student's *t*-test or a Fisher's Exact Test as indicated. To account for variability due to primary T cell culturing and donor source, statistical significance in experiments performed in primary lymphocytes was determined using a two-tailed, paired Student's *t*-test.

## RESULTS

### Generation of artificial transcription factors to control *CCR5* gene expression

To manipulate the expression of the *CCR5* gene, we generated TALE-based designer transcription factors. We firstly identified regions of open chromatin in human CD4+ T cells in the *CCR5* proximal promoter using DNase I hypersensitivity sites available in the UCSC Genome Browser database (<http://genome.ucsc.edu/>). Within these regions, we chose six target sites starting with a 5'-T nucleotide to fulfill TALE binding requirements (Figure 1A; Supplementary Table S1). We assembled the corresponding TALE domains using our optimized A4-NH scaffold (22,23). To assess binding efficiency to their intended target sites, we fused them with the VP16 transactivation domain (33), resulting in designer transcriptional activators (DTA). Co-transfection of the DTA expression plasmids and a reporter plasmid containing the Luciferase gene under the control of a minimal *CCR5* promoter (−320 to +1 bp relative to *CCR5* transcription start site) represented an optimal system to evaluate DNA binding capacity of the different TALEs. Three out of six DTAs were able to significantly induce Lu-

ciferase expression up to 4.5-fold over background (Supplementary Figure S1A). Simultaneous delivery of up to three different DTAs resulted in synergistic activity (Supplementary Figure S1B), as described before (34). To generate designer transcriptional repressors (DTRs) we switched the VP16 domain of the DTAs with a KRAB domain (35). Since HEK293T cells do not express CCR5, to dissect the activity of the six corresponding repressors (DTRs) we modified our reporter system to achieve basal level of reporter gene expression. Thereby, we fused the previously characterized CCR5 promoter fragment to a minimal CMV promoter (mCMV) driving the expression of an enhanced green fluorescent protein (EGFP, Figure 1A) and monitored DTR silencing ability via flow cytometry. The six DTRs were transfected into a surrogate reporter cell line stably expressing the reporter construct (HEK293T-EGFP) and seven days later, the reduction of EGFP expressing cells ranged from 10% to 20% for all repressors tested (Figure 1B). Interestingly, while the combination of two effectors showed a significant increase in silencing potency, the addition of a third repressor was rather deleterious, likely by counteracting the synergistic repression (Supplementary Figure S2A). Since DTR #6 repression was most consistent, subsequent experiments were carried out using the corresponding DNA binding domain unless specified otherwise. Long-term monitoring of the transfected reporter cells showed that EGFP levels returned to normal as expected from a transiently expressed DTR (Supplementary Figure S2B).

### Designer epigenome modifiers to stably silence target gene expression

To overcome transient gene silencing by DTRs, we engineered an effector capable of inducing potent and long-lasting silencing through the local recruitment of heterochromatin structures. We combined the KRAB repressor with a previously described single chain fusion of the C-terminal domains of the human *de novo* DNA methyltransferase 3A (DNMT3A) and of the murine regulatory factor DNA methyltransferase 3-like (Dnmt3L) (24) (Figure 1C). This single molecule was named designer epigenome modifier (DEM). A designer methyltransferase (DMT) was generated to evaluate the contribution of the sole methyltransferase component on silencing activity. DTR, DMT and DEM equipped with the same CCR5-targeting DNA binding domain #6 were delivered in the form of *in vitro* transcribed mRNA and able to reduce EGFP expression in the HEK293T-EGFP reporter cell line within a week (Figure 1C). While transient expression of both DTR #6 and DMT #6 resulted in modest and/or short-term EGFP silencing that was exhausted within three weeks, transient DEM #6 expression was sufficient to induce sustained EGFP silencing in more than 80% of the cells until the experiment was terminated 65 days post-transfection (Figure 1C). An inactive DMT (dDMT) that lacked the KRAB domain and harbored a catalytically inactive DNMT3A (25) did not affect EGFP expression and was used as a negative control (Figure 1C). Importantly, the same effector delivered in the form of plasmid resulted in significantly less EGFP silencing as compared to delivery via *in vitro* transcribed mRNA

(Figure 1D). To demonstrate that the high efficacy of the DEMs was based on its unique architecture that combined KRAB and DNA methyltransferase in a single molecule, the two effectors were fused to distinct DNA binding domains (i.e. #3 and #6, respectively). The split architecture showed robust and sustained EGFP silencing albeit at a significantly lower extent as compared to the single molecule DEM (Supplementary Figure S3). To confirm that EGFP silencing was a consequence of targeted CpG methylation, genomic DNA of HEK293T-EGFP cells was analyzed using bisulfite conversion at different time points following DEM #6 delivery. Two days after transfection, ~60% of the CpG diresidues were methylated in a 500 bp region centered around the DEM #6 binding site (Figure 2A, upper panel). Average methylation increased to 80% at day 6 after transfection and remained unaltered up to one month, highlighting the fast kinetics by which *de novo* methylation was induced by DEMs and maintained over time (Figure 2A, lower panel). Importantly, comparative DNA methylation analysis 31 days post transfection revealed that failure in achieving stable EGFP silencing mediated by DTR or DMT as compared to DEM was associated to a failure in depositing *de novo* DNA methylation at the target region (Supplementary Figure S4). To evaluate the spreading of DEM-induced methylation, we examined regions at increasing distances from the DEM #6 binding site via sequencing of bisulfite-converted genomic DNA one month after delivery of the DEM (Figure 2B). On average, about 80% of CpGs were methylated at up to 1-kb distance from the DEM #6 binding site while still about 33% of CpGs at a 2-kb distance were methylated, highlighting the high potency of the DEM platform to robustly induce sustained *de novo* methylation over a wide range. Reversibility of gene silencing was evaluated on EGFP-negative cells enriched by FACS and either transfected with DTA #6 or treated with the non-specific demethylating agent 5-Aza-2'-deoxycytidine (5-AZA). In both cases, EGFP expression was successfully reactivated (Supplementary Figure S5), indicating that DEM-induced silencing is reversible.

### Silencing of endogenous genes using designer epigenome modifiers is retained through cell division

To dissect the ability of DEMs to induce targeted gene silencing in a chromosomal context, we designed four novel DEMs targeted to the first exon or intron of the *CXCR4* gene (Figure 3A), which encodes the co-receptor used by T-tropic HIV strains and delivered them in the *CXCR4*-expressing cell line HEK293T. Two days later, *CXCR4* transcript and protein levels were reduced on average by 3.4- and 2.5-fold, respectively, as compared to controls (Figure 3B and C). Methylation analysis at the target site performed 20 days post DEM delivery revealed that, while only about 1% of CpGs were methylated in control cells, CpG methylation increased from ~1% to ~20% in cells expressing the most efficient *CXCR4*-specific DEM R2 (Figure 3D). To confirm that DEM efficacy in inducing gene silencing outperforms that of single effectors, we compared side-by-side the efficacy of *CXCR4*-specific DTR, DMT and DEM, respectively, all equipped with the most efficient *CXCR4*-specific DNA binding domain R2. Similarly to the results obtained

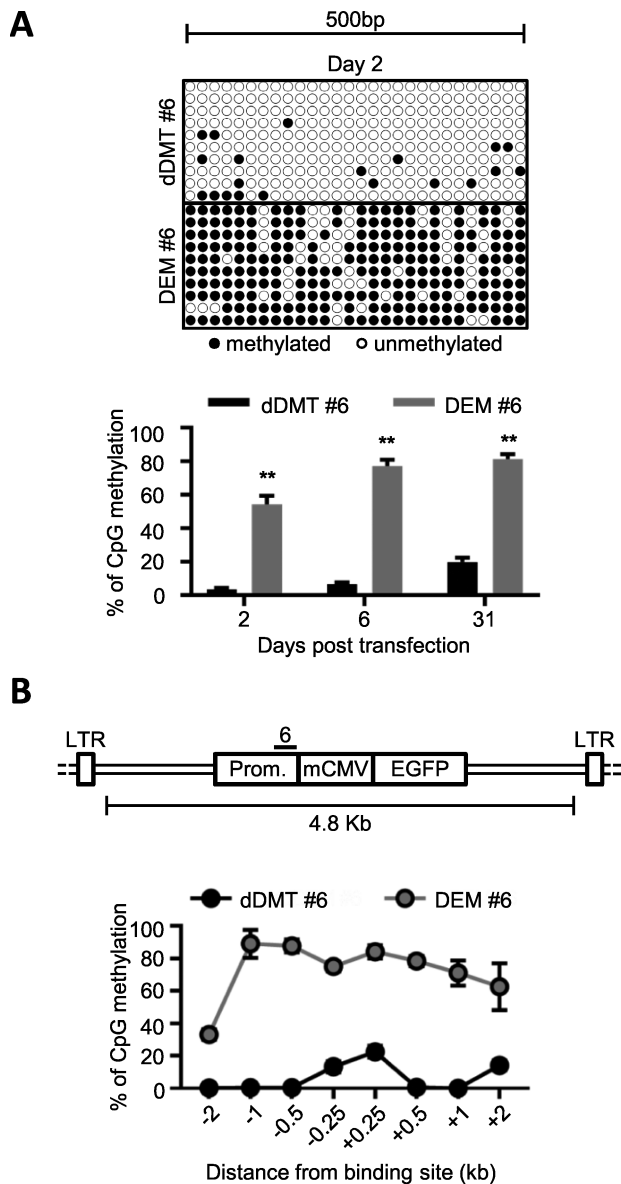


**Figure 2.** Potent CpG methylation induced by the DEMs. (A) Assessment of DEM-induced CpG methylation in a reporter cell line. HEK293T-EGFP reporter cells were transfected with DEM #6 or the inactive control and bisulfite sequencing performed on a region of 500 bp centered around the target site. Methylation analysis was carried out 2, 6 and 31 days post transfection. The methylation of individual CpGs within this region two days post transfection is depicted (top) and the overall methylation summarized in the histogram (bottom) (mean  $\pm$  S.E.M.). (B) Spreading of synthetic methylation. The extent of CpG methylation was measured up to a distance of 2-kb from the DEM target site within the integrated reporter (top) in HEK293T-EGFP cells thirty-one days following DEM #6 delivery. The distances in reference to the target site are indicated in the histogram (bottom) (mean  $\pm$  S.E.M.).

with the EGFP reporter, DTR-mediated *CXCR4* silencing was transient and was lost 20 days post-delivery. Even though DMT-mediated silencing was retained over time, DEM-induced *CXCR4* silencing was significantly higher both in short- and long-term analysis (Figure 3E), highlighting the importance of combining the three effectors in a single molecule. Having shown that DEM architecture

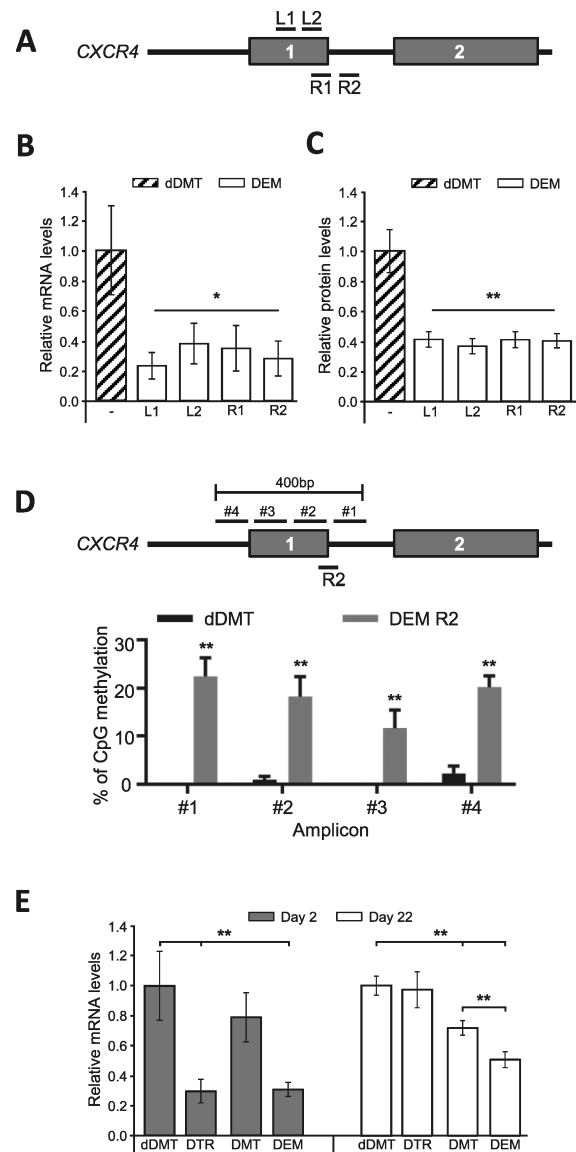


**Figure 3.** Stable silencing of the endogenous *CXCR4* gene. (A) Schematic of the *CXCR4* gene. Target sites bound by *CXCR4*-specific DEMs are indicated. L1 and L2 target the + strand while R1 and R2 target the - strand. Grey boxes represent *CXCR4* exons. (B, C) Assessment of *CXCR4* silencing. DNA transfections were carried out in HEK293T cells and analysis was performed two days post transfection. *CXCR4* mRNA (B) and protein (C) levels as determined by quantitative RT-PCR and flow cytometry respectively are depicted. The inactive dDMT targeting position L1 was used as a negative control. mRNA levels are expressed relative to *B2M*. Protein levels are expressed relative to the inactive control. (mean  $\pm$  S.E.M.,  $n = 6$  (B) and  $n = 5$  (C)). Statistical significance calculated with a two-tailed, paired Student's *t*-test (\* $P < 0.05$ ; \*\* $P < 0.01$ ). (D) *CXCR4* CpG methylation following DEM treatment. Cells were harvested 20 days post transfection and methylation assessed by bisulfite sequencing at a distance of -300 bp to +100 bp relative to the binding site R2 (mean  $\pm$  S.E.M.,  $n = 4$ ). The four indicated amplicons are shown to scale in the upper panel. Statistical significance was calculated with a two-tailed, paired Student's *t*-test (\* $P < 0.05$ ; \*\* $P < 0.01$ ). (E) Comparison of *CXCR4*-specific effectors activity. The histograms show the *CXCR4* expression levels upon delivery of DTR, DMT and DEM equipped with the *CXCR4*-specific DNA binding domain R2 at the indicated time points. *CXCR4* transcript levels, normalized to the housekeeping gene *B2M*, are expressed relative to the corresponding inactive control (dDMT; mean  $\pm$  S.E.M., experiments were performed three times in triplicate). Statistical significance calculated with a two-tailed, paired Student's *t*-test (\*\* $P < 0.01$ ).

is more efficient in inducing endogenous gene silencing as compared to the individual effectors, we used DEMs for the subsequent experiments in primary cells.

### Designer epigenome modifiers are able to effectively silence endogenous genes in primary human T cells

Having defined the optimal conditions to silence the *CCR5* and *CXCR4* genes in cell lines, we aimed at achieving gene silencing in primary human CD4<sup>+</sup> T cells, a relevant system to investigate the potential of DEMs for clinical translation (17). The best performing DEMs either targeting *CCR5* or *CXCR4* were delivered in the form of mRNA in pre-activated CD4<sup>+</sup> T lymphocytes isolated from healthy human donors (Figure 4A). Analysis of target gene expression levels four days upon nucleofection revealed that expression of *CCR5*-specific DEMs resulted in 1.8- or 1.6-fold reduction in *CCR5* transcript or protein levels, respectively, as measured by quantitative RT-PCR or flow cytometry (Figure 4B and E). Interestingly, in contrast to experiments in the reporter cell line, splitting the KRAB and the DNA methyltransferase activities into two distinct molecules failed to promote measurable target gene silencing, highlighting that the structure of DEMs is essential to achieve sustainable control of target gene expression in the chromosomal context (Supplementary Figure S6). *CXCR4*-specific DEMs had moderate effect on *CXCR4* expression (Figure 4C and F) at the first analyzed time point. This result may be expected since the basal expression levels of *CXCR4* are ~20-fold higher than the *CCR5* transcript levels (Supplementary Figure S7), and the short time between DEM delivery and analysis likely was not enough to lead to a measurable reduction of target gene expression. Eighteen days upon delivery of the DEMs, *CCR5* and *CXCR4* expression levels were measured again. The silencing effect at the *CCR5* gene was lost (Figure 4B, E), possibly because of the two necessary activation cycles to keep the primary T cells in culture or the lack of CpG islands in its promoter. On the other hand, silencing of *CXCR4* was increased, resulting in a significant 1.6-fold reduction both in *CXCR4* transcript and protein levels (Figure 4C and F). Importantly, more in-depth expression analysis by flow cytometry revealed that DEM delivery resulted in complete gene silencing in ~50% of the cells. In the remaining cells there was either no effect or only a partial gene silencing, as indicated by the reduction in mean fluorescence intensity values, likely due to partial methylation of the target gene promoter (Supplementary Figure S8).

Since ablation of a single HIV co-receptor does not protect from all HIV strains, there is an urgent need to develop strategies with broad protection from HIV infection. To demonstrate that the DEM platform is amenable for multiplexing in primary human T cells, DEM #6 and DEM R2 were co-expressed into pre-activated CD4<sup>+</sup> T lymphocytes. DEM multiplexing led to a significant 2.6- and 1.8-fold reduction in *CCR5* and *CXCR4* transcripts, respectively, and to about 2-fold reduction in the levels of both proteins at the indicated time points (Figure 4D and G) underlying that DEMs can be efficiently used to simultaneously silence multiple genes in primary human cells.

To confirm that the observed silencing was a consequence of DEM-mediated methylation, different regions of the *CCR5* and *CXCR4* promoters were analyzed by bisulfite sequencing. Next generation sequencing of amplicons at increasing distances from the DEM #6 binding site in the *CCR5* promoter of cells harvested 11 days after DEM delivery revealed a significant increase in CpG methylation up to a distance of about 1-kb from the DEM target site (Figure 4H; Supplementary Figure S9A). Sites further away did not show any difference in methylation (Supplementary Figure S9B). Similarly, at the *CXCR4* promoter 18 days after DEM delivery we measured up to 16-fold increase in *de novo* DNA methylation (Figure 4I). Chromatin immunoprecipitation revealed an increase in the repressive epigenetic mark H3K9me3 in close proximity of the corresponding DEM target sites at both promoters (Figure 4J and K). Overall, these data suggest that early establishment of repressive chromatin marks can result in sustained repression of target gene expression via CpG methylation.

### Safety profile of designer epigenome modifiers in primary human T lymphocytes

Proper evaluation of DEM safety requires profiling their specificity in clinically relevant cells. First, we measured the expression levels of neighboring genes within 200-kb from the DEM #6 binding site. Four days after DEM delivery, qRT-PCR analysis revealed no changes in their expression levels (Supplementary Figure S10). Subsequently, total RNA extracted from three independent experiments was subjected to whole transcriptome analysis via RNA-seq. In line with the qRT-PCR results (Figure 4B), *CCR5* transcript levels were reduced up to 1.7-fold while no differences were measured at the unrelated  $\beta$ 2-microglobulin (*B2M*) gene (Supplementary Figure S11). A more detailed analysis revealed 84 genes (including *CCR5*) that were consistently up- (28 genes) or down-regulated (56 genes) >1.5-fold (Supplementary Table S2). To verify whether the observed de-regulation was due to direct binding of DEM #6 at off-target sites, we identified all potential off-target sites harboring up to three mismatches as compared to the *CCR5* on-target sequence using the online COSMID tool (29) (Supplementary Table S3). Importantly, none of the predicted off-target sites was within 10-kb of the transcription start sites of the differentially regulated transcripts. We thereby concluded that the variations in gene expression measured by RNA-seq were unrelated to DEM off-target binding.

Further, we performed a whole genome accessibility assay based on a high-throughput Assay for Transposase-Accessible Chromatin (ATAC-seq) (32). This method captures regions of open chromatin and is indicative of differentially accessible regions, as a consequence of DEM activity (Figure 5A). Results from two independent experiments revealed lower chromatin accessibility at the *CCR5* promoter in a region of ~3.5-kb encompassing the *CCR5* DEM #6 binding site as compared to controls. On the other hand, accessibility at the unrelated *B2M* gene was unchanged (Figure 5B). Moreover, we identified 324 additional sites showing lower chromatin accessibility (Supplementary Table S4), however, none of these included any of the de-regulated

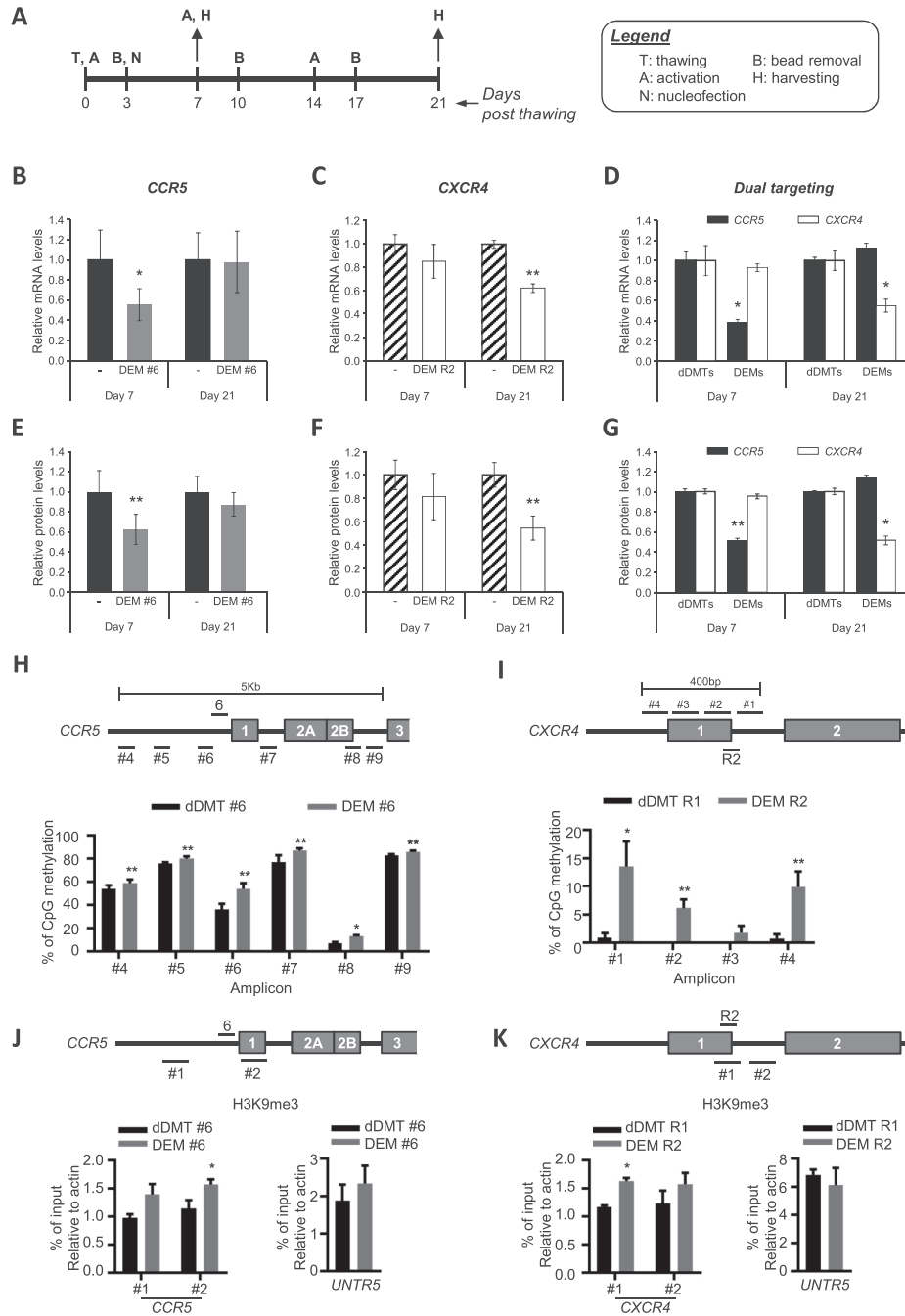


**Figure 4.** Functionality of DEMs at the *CCR5* and *CXCR4* genes in primary CD4<sup>+</sup> cells. (A) Time course of primary T cell experiments. After thawing (T), the cells were activated (A) with CD2/CD3/CD28 beads for 3 days. Beads were removed (B) prior to nucleofection (N) and 3 days after each successive reactivation. Cells were either harvested (H) for analysis or reactivated every 7 days. (B, C) Analysis of *CCR5* or *CXCR4* transcript (E, F) and protein levels following DEM mRNA nucleofection. Transcript levels, relative to *B2M*, and protein levels, determined via flow cytometry, are expressed relative to the corresponding inactive control (dDMT) indicated with ‘-’ (mean ± S.E.M., experiments were performed at least three times in triplicates). Statistical significance calculated with a two-tailed, paired Student’s *t*-test (\**P* < 0.05; \*\**P* < 0.01). (D, G) Analysis of *CCR5*- and *CXCR4*-specific DEMs. Transcript levels, relative to *B2M*, and protein levels, determined via flow cytometry, are expressed relative to the corresponding inactive control (dDMT) (mean ± S.E.M., experiments were performed three times in triplicate). Statistical significance calculated with a two-tailed, paired Student’s *t*-test (\**P* < 0.05; \*\**P* < 0.01). (H, I) Methylation analysis at the target sites. Next-generation bisulfite sequencing (H) or Sanger sequencing (I) were used to monitor the extent of DEM-induced CpG methylation in regions surrounding the respective DEM target site in *CCR5* or *CXCR4*, respectively, as indicated by horizontal bars depicting the analyzed amplicons. The positions of the amplicons are shown to scale with reference to the genomic locus and the respective DEM binding site. Schematic of the amplicons investigated is depicted (top) and the histogram summarizes the percentage of CpG methylation measured (bottom, mean ± S.E.M., *n* = 3). Statistical significance calculated with a two-tailed, homoscedastic Student’s *t*-test (\**P* < 0.05; \*\**P* < 0.01). (J, K) *CCR5* and *CXCR4* chromatin immunoprecipitation (ChIP). Schematic depicts the investigated regions (top) indicated by horizontal bars and shown to scale with reference to the genomic locus and the respective DEM binding site. Cells were harvested seven days post nucleofection and H3K9me3 ChIP analysis carried out. Results are expressed as the percentage of input relative to actin. UNTR5 was used as a positive control (mean ± S.E.M., *n* = 3). Statistical significance calculated with a two-tailed, paired Student’s *t*-test (\**P* < 0.05).

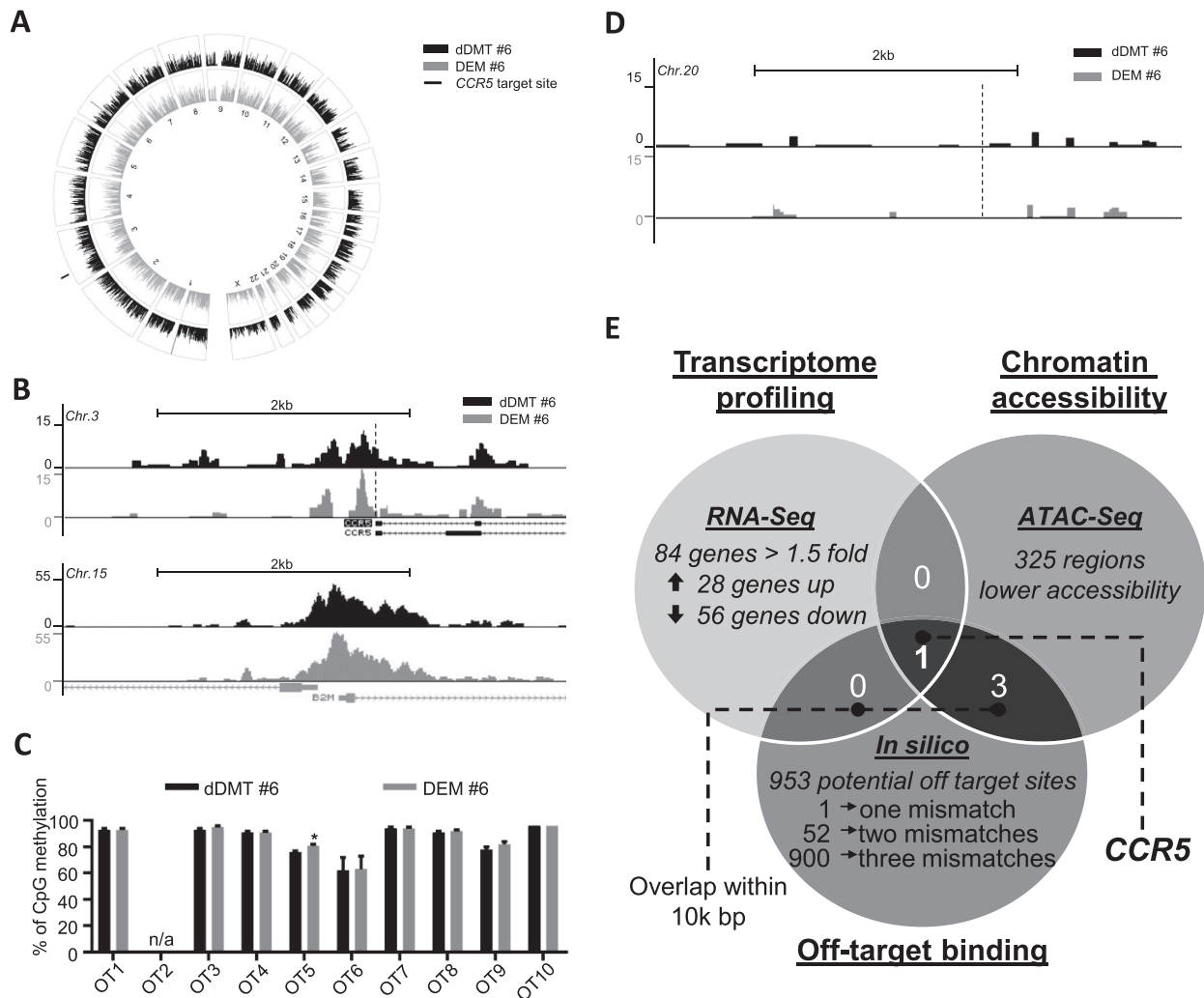


**Figure 5.** Specificity profile of DEMs. (A) ATAC-seq results. Circos plot showing whole genome accessibility in genomic DNA extracted from primary lymphocytes nucleofected either with DEM #6 (grey) or its inactive counterpart dDMT #6 (black). The line indicates the DEM #6 target site on chromosome 3 (*CCR5*). (B) Accessibility at *CCR5* (top) and *B2M* (bottom) in the indicated samples. Normalized read counts pooled from two independent experiments are shown. Dashed vertical line indicates DEM #6 binding site. (C) DEM off-target activity at predicted sites. The extent of CpG methylation at potential DEM #6 off-targets (OT) predicted *in silico* was analyzed via next generation bisulfite sequencing. For each region we analyzed the average CpG methylation in a single amplicon encompassing the predicted off-target site. Histogram shows the average CpG methylation measured (mean  $\pm$  S.E.M.,  $n = 3$ ). Statistical significance calculated with a two-tailed, paired Student's *t*-test (\* $P < 0.05$ ). n/a denotes failure in obtaining a PCR product. (D) Accessibility at the off-target OT5 measured via ATAC-seq. (E) Venn diagram showing the overlap between ATAC-seq, RNA-seq and *in silico* off-target sites predicted via PROGNOS. The number of overlapping sites is indicated. Overlap with computational prediction of off-target sites is restricted to hits within 10-kb distance from the annotated transcription start sites (TSS) of the 84 de-regulated genes identified via RNA-seq analysis or from the 325 regions of lower chromatin accessibility resulting from ATAC-seq analysis respectively.

genes identified by RNA-seq (Supplementary Table S2). Although 113 of these sites were located within 10-kb of transcription start sites of known genes (Supplementary Table S5), transcriptional profiling of the corresponding genes using RNA-seq revealed no significant differences in their expression levels (>1.5-fold) as compared to controls. Notably, three of the 324 regions showing lower chromatin accessibility had a predicted off-target site within 10-kb distance (Supplementary Table S6). Again, the closest genes were either not expressed or not de-regulated (Supplementary Table S6). To assess whether the lower accessibility regions identified via ATAC-seq can be linked to DEM off-target activity, we selected the top five regions of Supple-

mentary Table S4 closer to genes expressed in human T lymphocytes and analyzed DNA methylation at these tracts via bisulfite sequencing. As shown in Supplementary Figure S12, in control cells these regions were largely unmethylated as expected from promoter regions of actively transcribed genes. Importantly, bisulfite sequencing at these sites show similar DNA methylation levels in cells that received the *CCR5*-specific DEM, highlighting that the lower chromatin accessibility measured by ATAC-seq was not a result of DEM off-target activity. Lastly, we computationally predicted the top 10 potential off-target sites of the DNA binding domain included in DEM #6 using the TAL Effector Nucleotide Targeter 2.0 tool (28) (Table 1) and an-

alyzed these sites for evidence of increased CpG methylation via next generation bisulfite sequencing. For all but one site, we measured no difference in CpG methylation in samples treated with DEM #6 as compared to controls (Figure 5C). The single off-target site that showed increased CpG methylation is an intergenic region on chromosome 20 which is not accessible in the chromatin context of T cells as shown by ATAC-seq (Figure 5D). In conclusion, overlap between high-throughput datasets obtained from RNA-seq and ATAC-seq analysis with *in silico* prediction of potential off-target sites revealed that the only common hit was the target gene *CCR5* (Figure 5E). Taken together, these results highlight the benign safety profile of DEM #6 in primary human T cells and introduce DEMs as a novel and powerful platform for targeted gene silencing in clinically relevant applications.

## DISCUSSION

The recent boost in developing DNA targeting platforms has opened the possibility to explore genome editing approaches for a myriad of different applications. A recent milestone has been achieved by Dr. June's lab by providing human T cells with resistance to HIV infection by genetically inactivating the *CCR5* gene using designer nucleases (17). In this context, genotoxicity is still a matter of discussion and may preclude a widespread application of the technology. Epigenome editing is emerging as an alternative strategy to inactivate a selected gene. Manipulation of the epigenome is reversible and intrinsically less invasive as compared to genome editing because it does not change the DNA sequence. This suggests that also off-target effects are less disruptive since they may have a functional outcome only if off-target binding occurs within cis-regulatory regions that are active in the cells of interest.

Two decades of development have led to the establishment of designer methyltransferases capable of stably silencing target gene expression in human cells (24). Recently, the activity of epigenome modifiers was improved by synergizing the activity of three epigenetic effectors in primary cells at a surrogate reporter locus (21). However, manipulation of endogenous gene expression and a thorough safety profile of epigenome editors in clinically relevant cells are still lacking. In addition, multiple recent reports have shown that gene silencing through targeted epigenome editing is not always retained long-term (36,37). Hence, there is a need to develop a platform capable of sustained gene silencing through the targeted deposition of repressive epigenetic marks which are stably maintained. We have established a novel platform, named designer epigenome modifiers (DEMs), to selectively silence the expression of endogenous genes long-term with remarkable specificity. To investigate the potential of using epigenome editing for clinical applications, we dissected the activity and safety of DEMs in clinically relevant primary human cells. To facilitate delivery and promote the on-target recruitment and assembly of the convoluted multi-domain complex that controls gene expression, we combined three effector domains, namely the Krüppel-associated box (KRAB) and a single chain fusion of the C-terminal domains from the human *de novo* DNA methyltransferase 3A (DNMT3A) and the murine

regulatory factor DNA methyltransferase 3-like (Dnmt3L), in a single molecule. For target selectivity, DEMs comprise the highly specific DNA binding domain of transcription activator-like effectors (TALEs). Reporter cell lines were used to identify the most active DEMs targeting the promoter of either *CCR5* or *CXCR4*, two genes highly relevant in the field of HIV therapy as their silencing has been associated with acquired resistance to HIV infection. We demonstrated that DEMs robustly induce on target DNA methylation and that the signal spreads up to 2-kb distance from their corresponding binding sites (Figure 2B). In addition, our data showed that the all-in-one architecture of DEMs is crucial for the establishment of target gene silencing in primary cells (Supplementary Figures S3 and S5), representing an immediate advancement over platforms based on the simultaneous delivery of multiple epigenetic effectors (21). Moreover, the kinetics of DEM-induced *de novo* CpG methylation is rapid and stably maintained over cell division (Figure 2A). However, we noticed different efficiencies in inducing DNA methylation at a surrogate reporter as compared to an endogenous promoter (Figure 3D). Hence, the chromosomal context may strongly influence the process, and silencing of an artificially integrated reporter in a cell line is thus not necessarily indicative of subsequent activity at endogenous loci. Interestingly, delivery of DEMs resulted in efficient target gene silencing only when delivered in the form of mRNA that secures the short time expression of the epigenome modifier. Longer exposure to the DEM upon plasmid DNA delivery resulted in significantly lower efficacy (Figure 1D). This suggests that stable repressive chromatin marks are efficiently induced by recruiting the endogenous silencing machinery and that sustained DEM expression counteracts the correct on-target assembly of this complex resulting in less effective gene silencing.

Having identified the most promising DEMs to silence *CCR5* or *CXCR4*, we explored the potency of this technology in inducing target gene silencing in clinically relevant primary human T cells. Indeed, inactivation of these genes has been associated with protection from HIV infection, highlighting the therapeutic potential of our approach. Following DEM delivery, short-term analysis revealed significant reductions of both *CCR5* transcript and protein levels, underlining the robustness of the DEM platform in inducing gene silencing in primary human cells. However, effects on *CXCR4* were less pronounced, probably as consequence of its high expression levels as compared to *CCR5* (Supplementary Figure S7) that do not allow a measurable reduction in transcripts and protein levels four days upon DEM delivery. To measure the long-term effects of DEMs, we established a culturing protocol that allowed us to keep primary T cells in culture for multiple weeks by metabolically activating the cells on a weekly basis (Figure 4A). Analysis at 18 days post DEM delivery revealed that, while *CCR5* silencing was lost, the silencing signals initiated by *CXCR4*-specific DEMs three days after the first activation cycle were enhanced over time, resulting in sustained *CXCR4* repression which was resistant to cell divisions and metabolic activation. We speculate that loss of *CCR5*-silencing may be due to the lack of a CpG island in the corresponding *CCR5* promoter which is on the other hand present in the *CXCR4* promoter and may contribute to DEM-mediated silencing.

Simultaneous control of gene expression is a valuable approach not only in basic research but also with therapeutic perspective. RNA guided nucleases (RGNs) have been recently used to simultaneously inactivate both HIV co-receptors in primary human CD4+ cells to create lymphocytes broadly resistant to HIV (38). However, multiplexing RGNs activity may lead to deleterious genomic rearrangements (39) particularly using highly effective nucleases. Thereby, it may be safer to aim at simultaneous gene silencing without altering the DNA sequence. Our data suggest that DEMs can be used to simultaneously deposit repressive chromatin marks at multiple genomic sites and that a careful choice of the DEM target site in proximity to CpG islands may help to maximize the silencing effect at multiple genes.

The dissection of the safety is paramount for the exploitation of targeted epigenome editing approaches in clinically relevant systems. We have carried out an extensive profiling of off-target effects potentially due to promiscuous DEM activity by combining *in silico* prediction of potential off-target binding sites with results obtained from high-throughput techniques, such as RNA-seq and ATAC-seq. While on-target epigenome editing was consistently demonstrated, we did not find any evidence of direct off-target effects mediated by the activity of DEMs upon off-target binding. However, we cannot exclude that chromatin tridimensional structure may drive DEM-induced assembly of silencing complexes at off-target sites which are spatially close to the on-target site. This can be further analyzed by performing transcriptome analysis in cells transfected with DEMs targeting overlapping target sites and searching for common de-regulated transcripts. While it will be necessary in the future to investigate this aspect more closely, our current data suggest that promiscuous binding does not pose a concern when using DEMs and establish TALE-based designer epigenome modifiers as an efficient and remarkably specific platform to induce targeted epigenome editing in therapeutically relevant primary human cells.

Epigenetics represents a complex network of mechanisms that eventually results in tightly controlled gene expression. Multiple human disorders, including neurodevelopmental disorders, have been associated with aberrant epigenetic regulation. Non-specific epigenetic drugs are explored in the clinics to restore the deregulated expression of key genes but their broad activity poses safety concerns. We have established a novel platform, that we named designer epigenome modifiers (DEMs), capable of inducing epigenome changes in a targeted fashion. We show that DEMs, through specific modulation of DNA methylation and chromatin accessibility at their intended target site, are able to control target gene expression in clinically relevant primary human T cells with remarkable specificity. Importantly, primary cells, such as T lymphocytes, do not tolerate DNA transfection and the delivery of epigenome editors based on the CRISPR-dCas9 platform (40) is challenging. In this scenario, applicability is strongly hampered both by the lack of a commercial source of recombinant dCas9 protein fused to epigenome editor domains (needed for RNP delivery), or by the manufacturing cost for guide RNAs that are chemically modified to avoid rapid degradation when combined with *in vitro* transcribed mRNA encoding the

dCas9 fusion protein. With this respect, the single-molecule architecture of DEMs allow for straightforward and cost-effective delivery in sensitive primary cells, such as T lymphocytes, resulting in sustained target gene silencing. Understanding whether the synthetic epigenetic mark introduced by DEMs is stable in highly dynamic cells, such as hematopoietic stem cells, is certainly key to envision the therapeutic potential of this novel platform.

## DATA AVAILABILITY

RNA-seq and ATAC-seq datasets have been deposited in Gene Expression Omnibus (GEO) under the accession number GSE108030.

## SUPPLEMENTARY DATA

Supplementary Data are available at NAR Online.

## ACKNOWLEDGEMENTS

We thank Niko Langer, Jamal Alzubi, Melina El Gaz, Jana Block, Gediminas Drabavičius and Róża Pietrzycka for their excellent technical assistance and the FACS core facility of the Center for Chronic Immunodeficiency for the cell sorting experiments. Sequencing for ATAC-seq experiments was conducted at the Genomics Core Facility of the European Molecular Biology Laboratories (EMBL).

## FUNDING

German Federal Ministry of Education and Research [BMBF-01EO0803 to T.C. and C.M.]; Excellence Initiative of the German Research Foundation [GSC-4, Speermann Graduate School, to C.M. and T.C.] (in part). T.M. is a recipient of a fellowship from the German Academic Exchange Service (DAAD). Funding for open access charge: Own grant [01EO0803].

*Conflict of interest statement.* T.C. is a consultant for TRACR Haematology. S.D. is co-owner of siTOOLS Biotech GmbH, Martinsried.

## REFERENCES

1. Jaenisch, R. and Bird, A. (2003) Epigenetic regulation of gene expression: how the genome integrates intrinsic and environmental signals. *Nat. Genet.*, **33**(Suppl.), 245–254.
2. Dawson, M.A. (2017) The cancer epigenome: concepts, challenges, and therapeutic opportunities. *Science*, **355**, 1147–1152.
3. Smith, Z.D. and Meissner, A. (2013) DNA methylation: roles in mammalian development. *Nat. Rev. Genet.*, **14**, 204–220.
4. Falahi, F., Sgro, A. and Blancafort, P. (2015) Epigenome engineering in cancer: fairytale or a realistic path to the clinic? *Front. Oncol.*, **5**, 22.
5. Kelly, T.K., De Carvalho, D.D. and Jones, P.A. (2010) Epigenetic modifications as therapeutic targets. *Nat. Biotechnol.*, **28**, 1069–1078.
6. Szyf, M. (2015) Prospects for the development of epigenetic drugs for CNS conditions. *Nat. Rev. Drug Discov.*, **14**, 461–474.
7. Cano-Rodriguez, D. and Rots, M.G. (2016) Epigenetic editing: on the verge of reprogramming gene expression at will. *Curr. Genet. Med. Rep.*, **4**, 170–179.
8. Thakore, P.I., Black, J.B., Hilton, I.B. and Gersbach, C.A. (2016) Editing the epigenome: technologies for programmable transcription and epigenetic modulation. *Nat. Methods*, **13**, 127–137.

9. Chavez, A., Scheiman, J., Vora, S., Pruitt, B.W., Tuttle, M., E.P.R.I., Lin, S., Kiani, S., Guzman, C.D., Wiegand, D.J. *et al.* (2015) Highly efficient Cas9-mediated transcriptional programming. *Nat. Methods*, **12**, 326–328.
10. Mussolino, C., Sanges, D., Marrocco, E., Bonetti, C., Di Vicino, U., Marigo, V., Auricchio, A., Meroni, G. and Surace, E.M. (2011) Zinc-finger-based transcriptional repression of rhodopsin in a model of dominant retinitis pigmentosa. *EMBO Mol. Med.*, **3**, 118–128.
11. Huisman, C., van der Wijst, M.G., Falahi, F., Overkamp, J., Karsten, G., Terpstra, M.M., Kok, K., van der Zee, A.G., Schuurings, E., Wisman, G.B. *et al.* (2015) Prolonged re-expression of the hypermethylated gene EPB41L3 using artificial transcription factors and epigenetic drugs. *Epigenetics*, **10**, 384–396.
12. Bailus, B.J., Pyles, B., McAlister, M.M., O'Geen, H., Lockwood, S.H., Adams, A.N., Nguyen, J.T., Yu, A., Berman, R.F. and Segal, D.J. (2016) Protein delivery of an artificial transcription factor restores widespread Ube3a expression in an Angelman Syndrome mouse brain. *Mol. Ther.*, **24**, 548–555.
13. Segal, D.J., Goncalves, J., Eberhardy, S., Swan, C.H., Torbett, B.E., Li, X. and Barbas, C.F. 3rd (2004) Attenuation of HIV-1 replication in primary human cells with a designed zinc finger transcription factor. *J. Biol. Chem.*, **279**, 14509–14519.
14. Dykxhoorn, D.M. and Lieberman, J. (2005) The silent revolution: RNA interference as basic biology, research tool, and therapeutic. *Annu. Rev. Med.*, **56**, 401–423.
15. Grimm, D., Streetz, K.L., Lajling, C.L., Storm, T.A., Pandey, K., Davis, C.R., Marion, P., Salazar, F. and Kay, M.A. (2006) Fatality in mice due to oversaturation of cellular microRNA/short hairpin RNA pathways. *Nature*, **441**, 537–541.
16. Kim, H. and Kim, J.S. (2014) A guide to genome engineering with programmable nucleases. *Nat. Rev. Genet.*, **15**, 321–334.
17. Tebas, P., Stein, D., Tang, W.W., Frank, I., Wang, S.Q., Lee, G., Spratt, S.K., Surosky, R.T., Giedlin, M.A., Nichol, G. *et al.* (2014) Gene editing of CCR5 in autologous CD4 T cells of persons infected with HIV. *N. Engl. J. Med.*, **370**, 901–910.
18. Cornu, T.I., Mussolino, C. and Cathomen, T. (2017) Refining strategies to translate genome editing to the clinic. *Nat. Med.*, **23**, 415–423.
19. Hilton, I.B., D'Ippolito, A.M., Vockley, C.M., Thakore, P.I., Crawford, G.E., Reddy, T.E. and Gersbach, C.A. (2015) Epigenome editing by a CRISPR-Cas9-based acetyltransferase activates genes from promoters and enhancers. *Nat. Biotechnol.*, **33**, 510–517.
20. Rivenbark, A.G., Stolzenburg, S., Beltran, A.S., Yuan, X., Rots, M.G., Strahl, B.D. and Blancafort, P. (2012) Epigenetic reprogramming of cancer cells via targeted DNA methylation. *Epigenetics*, **7**, 350–360.
21. Amabile, A., Migliara, A., Capasso, P., Biffi, M., Cittaro, D., Naldini, L. and Lombardo, A. (2016) Inheritable silencing of endogenous genes by hit-and-run targeted epigenetic editing. *Cell*, **167**, 219–232.
22. Morbitzer, R., Elsaesser, J., Hausner, J. and Lahaye, T. (2011) Assembly of custom TALE-type DNA binding domains by modular cloning. *Nucleic Acids Res.*, **39**, 5790–5799.
23. Mussolino, C., Morbitzer, R., Lutge, F., Dannemann, N., Lahaye, T. and Cathomen, T. (2011) A novel TALE nuclease scaffold enables high genome editing activity in combination with low toxicity. *Nucleic Acids Res.*, **39**, 9283–9293.
24. Siddique, A.N., Nunna, S., Rajavelu, A., Zhang, Y., Jurkowska, R.Z., Reinhardt, R., Rots, M.G., Ragozin, S., Jurkowski, T.P. and Jeltsch, A. (2013) Targeted methylation and gene silencing of VEGF-A in human cells by using a designed Dnmt3a-Dnmt3L single-chain fusion protein with increased DNA methylation activity. *J. Mol. Biol.*, **425**, 479–491.
25. Li, F., Papworth, M., Minczuk, M., Rohde, C., Zhang, Y., Ragozin, S. and Jeltsch, A. (2007) Chimeric DNA methyltransferases target DNA methylation to specific DNA sequences and repress expression of target genes. *Nucleic Acids Res.*, **35**, 100–112.
26. Jiang, H., Lei, R., Ding, S.W. and Zhu, S. (2014) Skewer: a fast and accurate adapter trimmer for next-generation sequencing paired-end reads. *BMC Bioinformatics*, **15**, 182.
27. Dobin, A., Davis, C.A., Schlesinger, F., Drenkow, J., Zaleski, C., Jha, S., Batut, P., Chaisson, M. and Gingeras, T.R. (2013) STAR: ultrafast universal RNA-seq aligner. *Bioinformatics*, **29**, 15–21.
28. Doyle, E.L., Booher, N.J., Standage, D.S., Voytas, D.F., Brendel, V.P., Vandyk, J.K. and Bogdanove, A.J. (2012) TAL Effector-Nucleotide Targeter (TALE-NT) 2.0: tools for TAL effector design and target prediction. *Nucleic Acids Res.*, **40**, W117–W122.
29. Cradick, T.J., Qiu, P., Lee, C.M., Fine, E.J. and Bao, G. (2014) COSMID: a web-based tool for identifying and validating CRISPR/Cas off-target sites. *Mol. Ther. Nucleic Acids*, **3**, e214.
30. Magoc, T. and Salzberg, S.L. (2011) FLASH: fast length adjustment of short reads to improve genome assemblies. *Bioinformatics*, **27**, 2957–2963.
31. Li, H. and Durbin, R. (2009) Fast and accurate short read alignment with Burrows-Wheeler transform. *Bioinformatics*, **25**, 1754–1760.
32. Buenrostro, J.D., Giresi, P.G., Zaba, L.C., Chang, H.Y. and Greenleaf, W.J. (2013) Transposition of native chromatin for fast and sensitive epigenomic profiling of open chromatin, DNA-binding proteins and nucleosome position. *Nat. Methods*, **10**, 1213–1218.
33. Seipel, K., Georgiev, O. and Schaffner, W. (1992) Different activation domains stimulate transcription from remote ('enhancer') and proximal ('promoter') positions. *EMBO J.*, **11**, 4961–4968.
34. Maeder, M.L., Linder, S.J., Reyon, D., Angstman, J.F., Fu, Y., Sander, J.D. and Joung, J.K. (2013) Robust, synergistic regulation of human gene expression using TALE activators. *Nat. Methods*, **10**, 243–245.
35. Margolin, J.F., Friedman, J.R., Meyer, W.K., Vissing, H., Thiesen, H.J. and Rauscher, F.J. 3rd (1994) Kruppel-associated boxes are potent transcriptional repression domains. *Proc. Natl. Acad. Sci. U.S.A.*, **91**, 4509–4513.
36. Kungulovski, G., Nunna, S., Thomas, M., Zanger, U.M., Reinhardt, R. and Jeltsch, A. (2015) Targeted epigenome editing of an endogenous locus with chromatin modifiers is not stably maintained. *Epigenet. Chromatin*, **8**, 12.
37. O'Geen, H., Ren, C., Nicolet, C.M., Perez, A.A., Halmai, J., Le, V.M., Mackay, J.P., Farnham, P.J. and Segal, D.J. (2017) dCas9-based epigenome editing suggests acquisition of histone methylation is not sufficient for target gene repression. *Nucleic Acids Res.*, **45**, 9901–9916.
38. Yu, S., Yao, Y., Xiao, H., Li, J., Liu, Q., Yang, Y., Adah, D., Lu, J., Zhao, S., Qin, L. *et al.* (2017) Simultaneous knockout of CXCR4 and CCR5 genes in CD4+ T cells via CRISPR/Cas9 confers resistance to both X4- and R5-tropic human immunodeficiency virus type 1 infection. *Hum. Gene Ther.*, **29**, 51–67.
39. Mussolino, C., Alzubi, J., Fine, E.J., Morbitzer, R., Cradick, T.J., Lahaye, T., Bao, G. and Cathomen, T. (2014) TALENs facilitate targeted genome editing in human cells with high specificity and low cytotoxicity. *Nucleic Acids Res.*, **42**, 6762–6773.
40. Vojta, A., Dobrinic, P., Tadic, V., Bockor, L., Korac, P., Julg, B., Klasic, M. and Zoldos, V. (2016) Repurposing the CRISPR-Cas9 system for targeted DNA methylation. *Nucleic Acids Res.*, **44**, 5615–5628.